Photodetachment of hydrogen anion inside a square torus microcavity

SHAO-HAO CHENG, DE-HUA WANG*, JIE DU
School of Physics and Optoelectronic Engineering, Ludong University, Yantai 264025, China

The photodetachment of hydrogen anion inside a microcavity in the shape of a concentric square torus is studied for the first time. Compared to the photodetachment of hydrogen anion inside a square microcavity, the classical motion of the detached electron becomes much more complex and chaos appears. We thoroughly find out the closed orbit of the detached electron and calculate the photodetachment cross section of this system. It is shown that oscillatory structure appears in the photodetachment cross section, which is caused by the quantum interference effects of the returning electron waves traveling along the closed orbits with the outgoing waves. In order to explore the quantum and classical correspondence in the square torus microcavity, we calculate the Fourier-transformed photodetachment cross section and find each peak in the Fourier-transformed cross section corresponds to the length of one detached electron's closed orbit. As a demonstration, the case for a concentric square torus with the side ratio of the inner and outer square equals to 0.5 is calculated and analyzed in detail. We hope that our results will be useful in understanding the photodetachment of anions or electron transport in a microcavity.

(Received September 30, 2015; accepted September 29, 2016)

Keywords: Photodetachment, Square torus microcavity, Anion

1. Introduction

Recently, with the development of the photodetachment microscopy and the surface physics, the photodetachment of anions near surfaces or in a microcavity have attracted a lot of attention[1-15]. In 2006, Yang, and Du et al first studied the photodetachment of H^- near a reflecting surface based on the closed orbit theory[1-2]. At the same time, Hansen and coworkers studied the chaotic transport and escape of microwaves from a two-dimensional vase-shaped cavity. They demonstrated that the geometrical structure of the cavity can significantly affect the escape of the waves. The vase cavity is a simple system in which the dynamics shows all the complexity of chaotic transport and on which clean and precise measurement can be made[16-18]. Besides, this system can simulate other more complex systems, such as the photodetachment of negative ion in parallel electric and magnetic fields or in a cavity[19,20,21]. Recently, Zhao and Du studied the photodetachment process of H^- anion inside a wedge shaped cavity[21]. It has been shown that the wedge cavity induces significant oscillations in the total escapes rates because of the quantum interference effects. In these early studies, the researches all studied the photodetachment of negative ion near surfaces or inside an open cavity. In 2012, our group began to study the photodetachment of H^- anion inside a closed microcavity. Firstly, we studied the photodetachment of H^- anion inside a square or a circular microcavity[22-23]. As we all know, square or circular microcavity is a very simple model. In order to further probe the correspondence between the quantum mechanics and the classical mechanics, we extend the analyses of these simple systems to a more complex system. We studied the photodetachment of H^- anion inside an annular microcavity[24]. Then what will happen if we put the H^- anion inside a square torus microcavity? Does the quantum and classical correspondence still exist in the square torus microcavity?

In this work, we study the photodetachment of H^- anion inside a square torus microcavity in the frame work of the semiclassical closed orbit theory for the first time. We still consider the surfaces of the square torus microcavity as elastic ones, and neglect the interaction between the detached electron and the microcavity [22-24]. The trajectory of the detached electron inside the microcavity is a straight line until it is reflected by the surfaces of the microcavity, and the reflection is elastic. Therefore, the electron reflects between the internal and external surfaces of the microcavity can be considered as a square torus billiard [25]. In comparison with the square microcavity[22], the detached electron's closed orbits in the square torus microcavity have a far richer structure. Chaotic behaviors appear in the detached electron's movement. We thoroughly search out the closed orbits of the detached electron in the square torus microcavity and calculate the photodetachment cross section in detail. Our study confirms that quantum and classical correspondence still exist in the square torus microcavity.

The plan of this paper is organized as follows. In section 2, we search out the closed orbits of the detached electron inside a square torus microcavity. A formula for calculating the photodetachment cross section is also put forward. In section 3, taking a concentric square torus with the side ratio of the inner and outer square equals to 0.5 as an example, we calculate and analyze the photodetachment cross section. Conclusions and perspective are given in section 4. Atomic units which are abbreviated as "a.u." are used unless indicated otherwise.

2. Theory and quantitative formula

2.1. Physical picture description

The schematic plot of the photodetachment of hydrogen anion inside a square torus microcavity is shown in Fig.1. The square torus microcavity can be considered as a constitution of an outer square boundary plus an inner square hole. Suppose the length of the outer side of the square torus is a , the inner side is b, $b=fa$ ($0 < f < 1$). The concentric square torus microcavity is placed in the x-y plane, with x-axis parallel to the horizontal side. The H^- ion is assumed to be at the origin, which located at the middle of the left side. As we all know, H^- ion is composed of a hydrogen atom and an electron. The binding potential between the electron and the hydrogen atom is very weak. When a laser light is irradiated on the H^- ion, the binding electron will be photo-detached. The H^- ion provides a coherent source of electrons wave propagating out from the location of the ion. The detached electron waves propagate in the form of the quantum waves along the classical trajectory. Inside the square torus microcavity, the electron trajectories follow straight line until they are bounced back by the inner or outer surfaces of the microcavity. At last, the electron may return to the origin of the negative ion after multiple bounces with the surfaces of the microcavity. Those electron trajectories that emit from the origin and finally return to it are called the closed orbits[26]. The interference effect between the returning electron waves with the outgoing source waves produces the oscillatory structure in the photodetachment cross section. Three detached-electron's trajectories inside a square torus microcavity are shown in Fig.1. The red line denotes a closed orbit. From this figure, we find as the outgoing angle of the detached electron is changed a little, the position of the returning point will deviate a lot, which suggests that the motion of the electron in the square torus microcavity is chaotic.

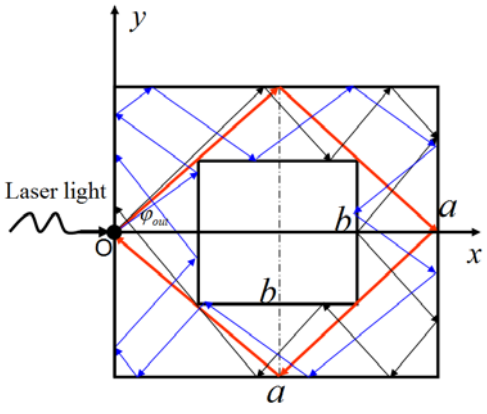

Fig.1(color online). Schematic illustration of the photodetachment of H^- ion inside a square torus microcavity. The H^- lies at the origin and the mircorcavity is in the x-y plane. Three detached electron trajectories propagating away from the origin and finally returning to the vicinity of the origin after being reflected several times by the inner and outer surfaces of the microcavity are shown. The closed orbit is marked by the red line. The outgoing angle of each trajectory relatives to x-axis is denoted as φ_{out} .

2.2. Closed orbits search

Because the electron trajectories are reflected by the surfaces of the microcavity, it is obvious that all the closed orbits that emit from the position of the negative ion and later return to it must be confined in the square torus microcavity. In order to find the closed orbits in the microcavity, we launch a large number of trajectories going out from the origin and keep track of the trajectories as they propagate and get reflected inside the microcavity. As a demonstration, we choose a concentric square torus with the side ratio of the inner and outer square equals to 0.5, b=0.5a. In comparison with the detached electron's movement in the square microvacity[22], the motion of the electron in the square torus microcavity becomes much complex. By careful search, we find the closed orbits can be separated into the following several types.

The first kind of closed orbit is very simple. The electron leaves the atom along the x-axis with the outgoing angle $\varphi_{out} = 0$, after being reflected by the inner surface of the square torus, it then retraces back to the atom. This orbit is called the "direct orbit". The length of this kind of closed orbit is $L^{(1)}$=0.5a. The direct orbit is shown in Fig.2.

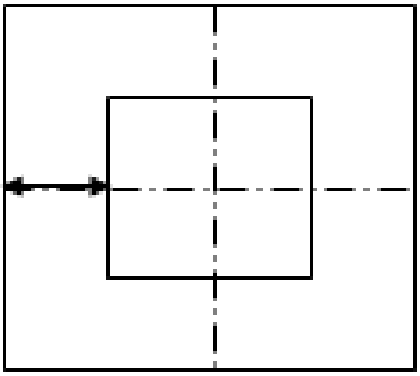

Fig.2. The first kind of closed orbit in the concentric square microcavity.

The second kind of closed orbit can be described as follows: the electron emits from the origin with the outgoing angle $0 < \varphi_{out} < 45^0$. Firstly, it bounces back by the left side of the inner square torus, then collides with the left side of the outer square, after reflecting by the inner and outer surfaces of the microcavity several times, it reaches the middle point of the upper side of the outer square. Due to the symmetry of the square torus microcavity, the electron can finally returns to the origin and forms a closed orbit. We use a parameter p_1 to distinguish different closed orbit. p_1 is a positive integer (p_1=2,5,6,9,10……), which satisfies the condition int[p_1/2]=odd number, where the symbol "int" denotes the round-off integer function. The length of this kind of closed orbit is:

$$L^{(2)} = 2a\sqrt{1+p_1^2} \tag{1}$$

The outgoing angle of the electron relative to the x-axis for each closed orbit is:

$$\tan\varphi_{out} = \frac{1}{p_1}.$$

The corresponding returning angle of each closed orbit is: $\varphi_{ret} = \pi - \varphi_{out}$. Some of this kind of closed orbit is given in Fig. 3. For example, Fig.3(a) shows the closed orbit with p_1=2, which leaves the atom with the outgoing angle $\varphi_{out} = 26.56^0$, after reflecting by the inner and outer surfaces of the square torus microcavity 11 times, it finally returns back to the atom. Fig.3(b) shows the closed orbit with p_1=5. The electron leaves the atom at an outgoing angle $\varphi_{out} = 11.31^0$, before it finally returns back to the atom, it has been reflected by the surfaces of the square torus microcavity 23 times. Similar descriptions can be given to the other closed orbits.

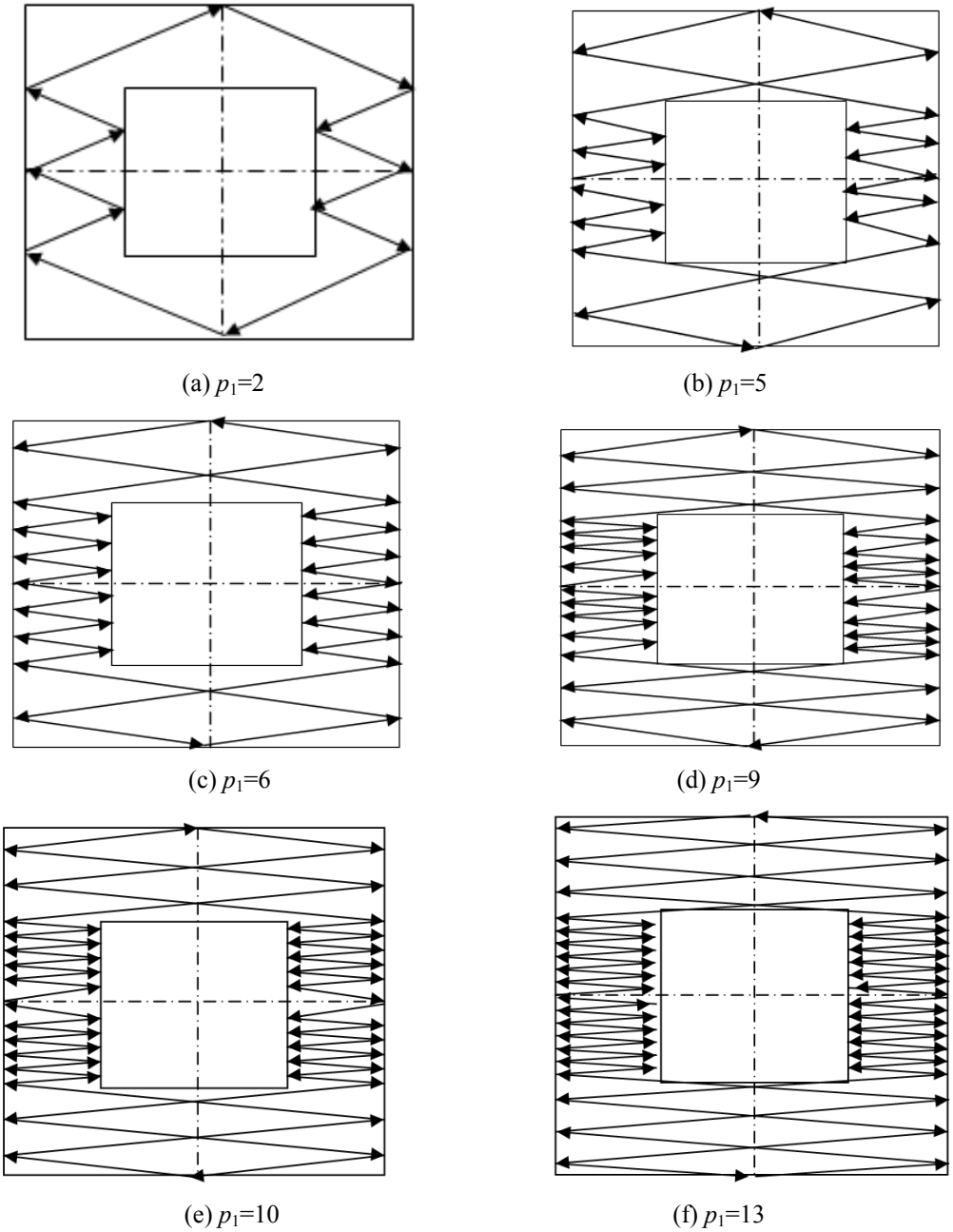

(a) p_1=2 (b) p_1=5

(c) p_1=6 (d) p_1=9

(e) p_1=10 (f) p_1=13

Fig.3. The second kind of closed orbit in the concentric square microcavity.

The third kind of closed orbit is as follows: the

electron emits from the origin with the outgoing angle $45^0 \le \varphi_{out} < 90^0$, firstly, it bounces back by the up side of the outer square torus, then the up side of the inner square. Finally, it reaches the middle point of the upper side of the outer square. Due to the symmetry of the square torus microcavity, the electron can return to the origin. We use a parameter p_2 to denote different closed orbit, p_2=1,2,5,6,9,10……. The length of this kind of closed orbit is :

$$L^{(3)} = 2a\sqrt{1+p_2^2} \ . \tag{2}$$

The outgoing angle of the electron is: $\tan\varphi_{out} = p_2$. The returning angle for each closed orbit is: $\varphi_{ret} = \pi - \varphi_{out}$. Some of this kind of closed orbits is given in Fig. 4.

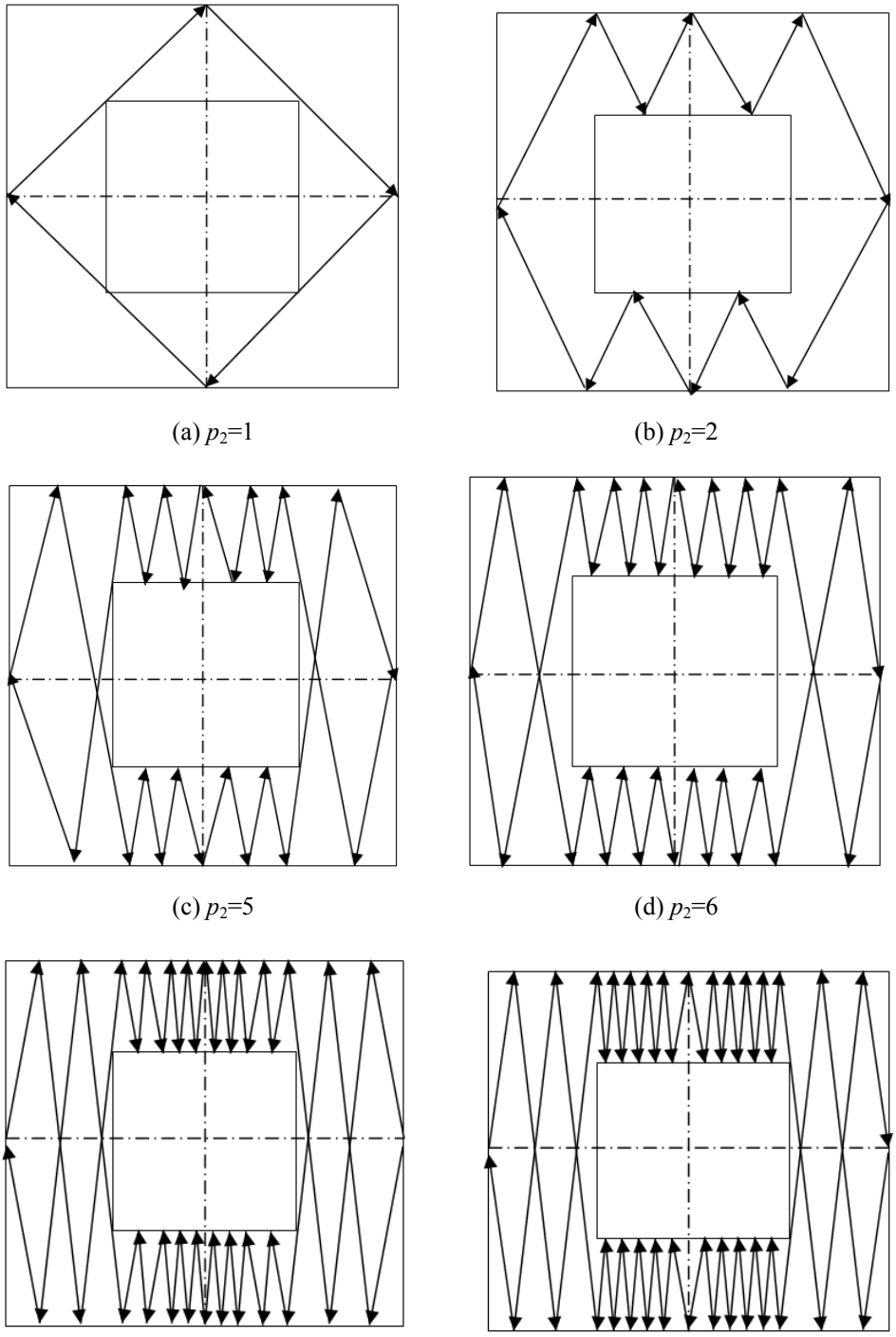

(a) p_2=1 (b) p_2=2

(c) p_2=5 (d) p_2=6

(e) p_2=9 (f) p_2=10

Fig.4. The third kind of closed orbit in the concentric square microcavity.

The fourth kind of closed orbit satisfies the following condition: the electron emits from the origin with the outgoing angle $45^0 \le \varphi_{out} < 90^0$. At first, it bounces back by the up side of the outer square torus, then the up side of the inner square, after bouncing back by the surfaces of the microcavity several times, it reaches the middle point of the upper side of the inner square. At last, the electron returns to the origin due to the symmetry of the square torus microcavity. We use a parameter p_3 to label different closed orbit. p_3 is a positive integer, p_3=3, 5, 11, 13, 19, 21…. The length of this kind of closed orbit is:

$$L^{(4)} = a\sqrt{4 + p_3^2} \tag{3}$$

The outgoing angle of the electron corresponds to this kind of closed orbit is: $\tan\varphi_{out} = p_3 / 2$. The returning angle for each closed orbit is: $\varphi_{ret} = \pi - \varphi_{out}$. Some of this kind of closed orbits is given in Fig. 5.

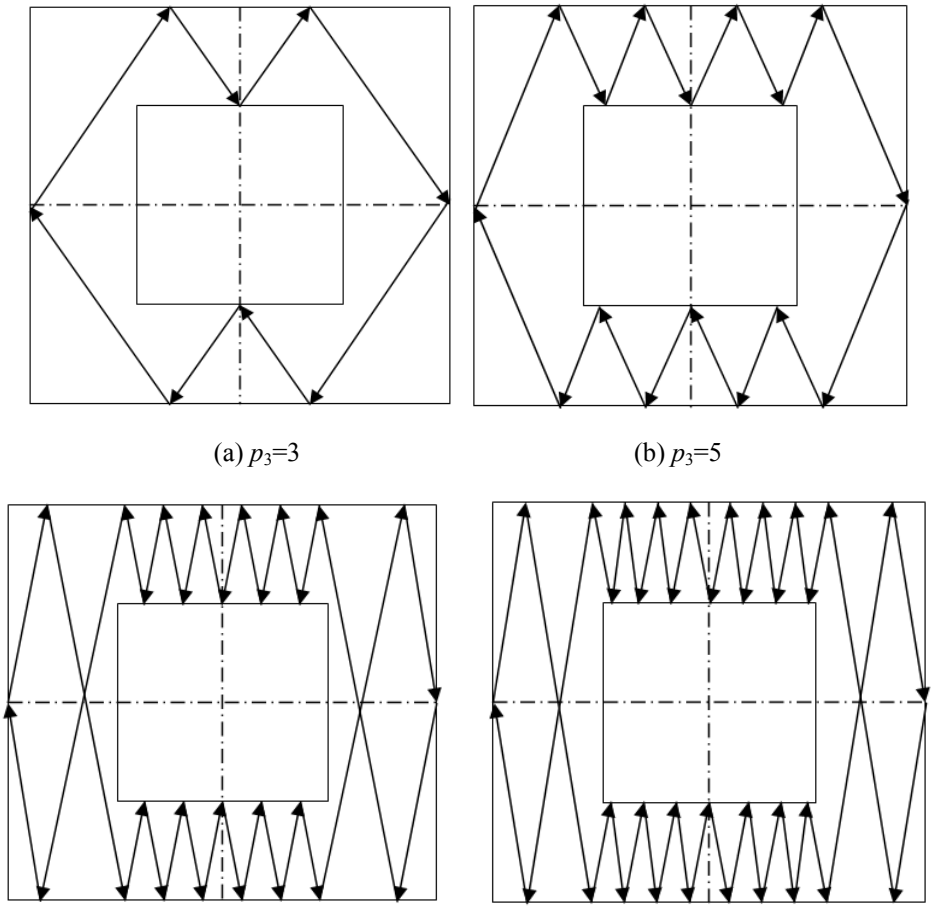

(a) p_3=3 (b) p_3=5

(c) p_3=11 (d) p_3=13

Fig.5. The fourth kind of closed orbit in the concentric square microcavity.

The fifth kind of closed orbit is as follows: the electron emits from the origin with the outgoing angle $0^0 < \varphi_{out} < 45^0$, firstly, it bounces back by the left side of the inner square torus, then the left side of the outer square, after bouncing back by the surfaces of the microcavity several times, it reaches the top-right corner of the square torus. At last, the electron retraces back to the origin. We use a positive integer p_4 to label different closed orbit, which satisfies p_4=3, 4, 11, 12, 19, 20…. The length of this kind of closed orbit is :

$$L^{(5)} = a\sqrt{1 + p_4^2} \tag{4}$$

The outgoing angle of the electron for this kind of closed orbit is: $\tan\varphi_{out} = 1/p_4$. The returning angle for each closed orbit is: $\varphi_{ret} = \pi + \varphi_{out}$. Some of this kind of closed orbits is given in Fig. 6.

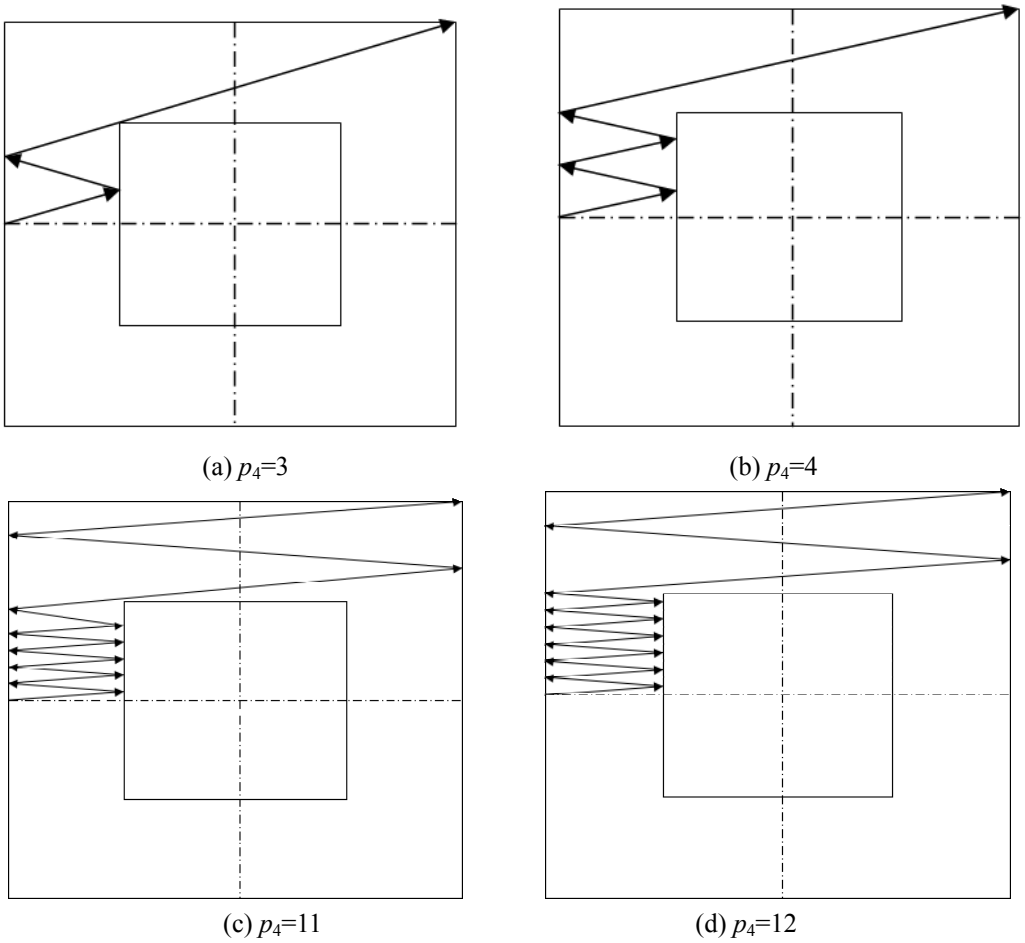

(a) p_4=3 (b) p_4=4

(c) p_4=11 (d) p_4=12

Fig.6. The fifth kind of closed orbit in the concentric square microcavity.

The sixth kind of electron's closed orbit emits from the origin with the outgoing angle $0^0 < \varphi_{out} < 45^0$, after bouncing back by the inner and outer surfaces of the microcavity several times, it reaches the left-right corner of the square torus. At last, the electron retraces back to the origin. We use a positive integer p_5 to distinguish different closed orbit, which satisfies p_5=7, 8, 15, 16, 23, 24…. The length of this kind of closed orbit is:

$$L^{(6)} = a\sqrt{1+p_5^2} \tag{5}$$

The outgoing angle of the electron for this kind of closed orbit is: $\tan\varphi_{out} = 1/p_5$. The returning angle for each closed orbit is: $\varphi_{ret} = \pi + \varphi_{out}$. Some of this kind of closed orbits is given in Fig. 7.

The outgoing angle of the seventh kind of closed orbit satisfies $45^0 < \varphi_{out} < 90^0$, after emitting from the origin, it is first bounced back by the upper surface of the microcavity, then it impacts the lower surface. After bouncing back by the upper and lower surfaces of the microcavity several times, it reaches the middle point of the left inner surface of the square torus.

Due to the symmetry of the square torus microcavity, the electron returns to the origin at last. We use a positive integer p_6 to distinguish different closed orbit, which satisfies p_6=1, 2, 3, 4, 5, 6…. The length of this kind of closed orbit is : $L^{(7)} = \frac{a}{2}\sqrt{1+16p_6^2}$. The outgoing angle of the electron for this kind of closed orbit is: $\tan\varphi_{out} = 4p_6$. The returning angle for each closed orbit is: $\varphi_{ret} = \pi - \varphi_{out}$. Some of this kind of closed orbits is given in Fig. 8.

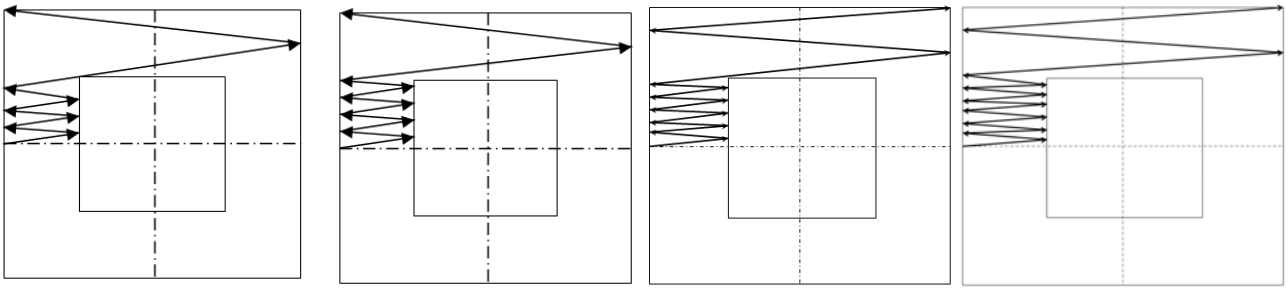

(a) p_5=7 (b) p_5=8 (c) p_5=15 (d) p_5=16

Fig.7. The sixth kind of closed orbit in the concentric square microcavity.

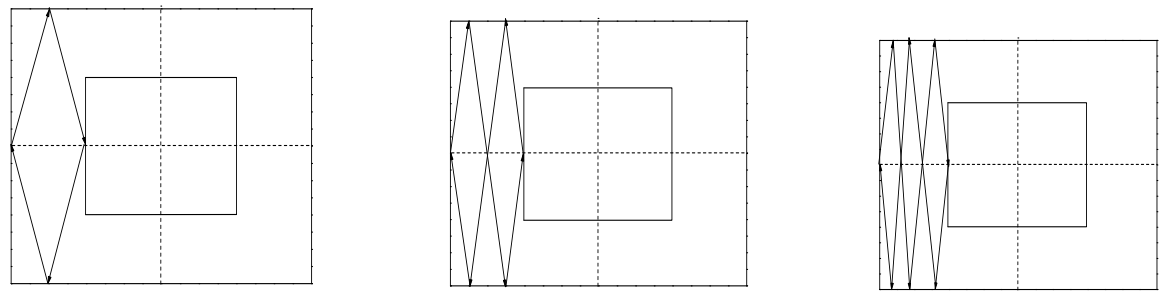

(a) p_6=1 (b) p_6=2 (c) p_6=3

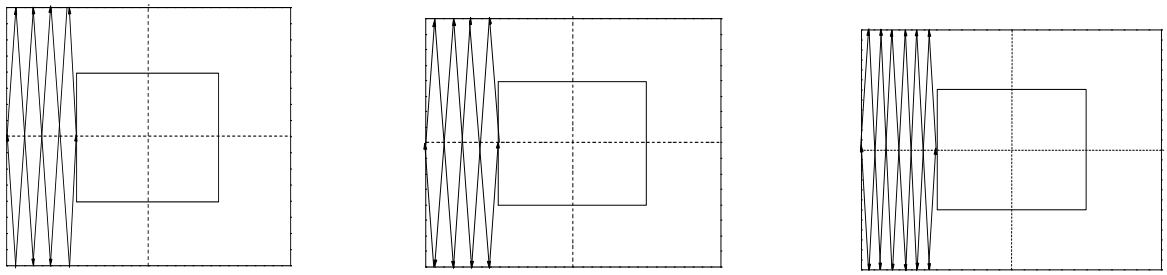

(d) p_6=4 (e) p_6=5 (f) p_6=6

Fig.8. The seventh kind of closed orbit in the concentric square microcavity.

In our calculation, we suppose the outer side of the square torus microcavity a=100a.u.. In table I, we summarize the integers p_1-p_6 and the length L of the above sixth kinds of closed orbit with the length L≤3000a.u.. Due to the symmetry of the square torus microcavity, we only give out the closed orbit with the outgoing angle $0 \le \varphi_{out} \le 90^0$. The length and the integer p_1-p_6 for those closed orbits with $-90^0 < \varphi_{out} \le 0^0$ are the same as the ones listed above.

Table I. Geometric parameters of the closed orbits inside a square torus microcavity, b=0.5a.

second kind		third kind		fourth kind		fifth kind		sixth kind		seventh kind	
p_1	$L^{(2)}$(a.u.)	p_2	$L^{(3)}$(a.u.)	p_3	$L^{(4)}$(a.u.)	p_4	$L^{(5)}$(a.u.)	p_5	$L^{(6)}$(a.u.)	p_6	$L^{(7)}$(a.u.)
2	447.21	1	282.84	3	360.55	3	316.22	7	707.10	1	206.16
5	1019.80	2	447.21	5	538.51	4	412.31	8	806.22	2	403.11
6	1216.55	5	1019.80	11	1118.03	11	1104.53	15	1503.33	3	602.08
9	1811.08	6	1216.55	13	1315.29	12	1204.16	16	1603.12	4	801.56
10	2009.98	9	1811.08	19	1910.49	19	1902.63	23	2302.17	5	1001.25
13	2607.68	10	2009.98	21	2109.50	20	2002.50	24	2402.08	6	1201.04
14	2807.13	13	2607.68	27	2707.39	27	2701.85			7	1400.89
		14	2807.13	29	2906.89	28	2801.78			8	1600.78
										9	1800.69
										10	2000.62
										11	2200.57
										12	2400.52
										13	2600.48
										14	2800.44

2. 3. Photodetachment cross section

According to the closed orbit theory, the photodetachment cross section of H^- ion in the external environment can be written as:

$$\sigma(E) = \sigma_0(E) + \sigma_{osc}(E) \tag{6}$$

In which $\sigma_0(E) = \dfrac{16\sqrt{2}\pi^2 B^2 E^{3/2}}{3c(E_b + E)^3}$ is the smooth background term of H^- in free space [21], E is the energy of the detached electron, $E_b = 0.754eV$ is the binding energy, B=0.31552 is a normalization constant, c is the light speed. $\sigma_{osc}(E)$ is the oscillating term, which is dependent on the external environment. Since the photodetachment process of H^- ion in the square torus microcavity is similar to the photodetachment process in the square or circular microvavity[22-23]. Therefore, we can use the same procedure to derive the oscillating term in the photodetachment cross section. For simplicity, we briefly give out some main formula.

The oscillating term $\sigma_{osc}(E)$ in Eq. (6) corresponds to the contribution of the overlap integral of the returning electron wave traveling along the closed orbits with the initial outgoing wave:

$$\sigma^{osc}(E) = -\frac{4\pi}{c}(E + E_b)\,\mathrm{Im} < D\psi_i \mid \psi_{ret} >, \tag{7}$$

where $\psi_i(\vec{r}) = \dfrac{Be^{-k_b r}}{r} = R(r)$ is the detached electron's initial wave function. D is the dipole operator, which is depended on the laser polarization[27].

$$\mid D\psi_i >= rR(r)\chi(\theta,\varphi), \tag{8}$$

$\chi(\theta,\varphi)$ is the angular factor. Assuming the laser light is linearly polarized in the x-y plane. Then for x-polarized laser light, $\chi_x(\theta,\varphi) = \sin\theta\cos\varphi$; for y-polarized laser light, $\chi_y(\theta,\varphi) = \sin\theta\sin\varphi$.

ψ_{ret} is the returning electron wave function caused by the reflection of the microcavity surfaces. In order to obtain the returning wave function along each closed orbit, we draw a small sphere around the ion with the radius $R_0 \approx 5.0a_0$. Then the outgoing wave on this sphere surface can be written as[28]:

$$\psi_{out}(R_0,\theta_{out},\varphi_{out}) = \frac{4Bk^2 i}{(k_b^2 + k^2)^2}\frac{e^{ikR}}{kR_0}\chi(\theta_{out},\varphi_{out}) \tag{9}$$

When this wave propagates out of the sphere surface and propagates in the square torus microcavity along the

closed orbit, its phase and amplitude will be changed. A phase loss π in the wave function will appear after each reflection by the surfaces of the microcavity. Once we have found the closed orbits of the detached electron, we are ready to construct the wave function according to the semiclassical approximation. The returning wave ψ_{ret} can be written as a sum of the above outgoing waves travelling along the closed orbits:

$$\psi_{ret}(r,\theta,\varphi)=\sum_j \psi_{out}(r,\theta,\varphi)A_j e^{i[S_j-\mu_j\pi]}, \tag{10}$$

A_j is the amplitude of the wave function, which is a ratio of Jacobians in the representation $(x(t,\theta,\varphi),y(t,\theta,\varphi))$, where x and y are the position of a classical trajectory as a function of time and initial launch angle of the j-th trajectory: $A_j=\left|J_j(t=0)/J_j(t)\right|^{1/2}$. $J_j(t)$ is the Jacobian: $J_j(t)=\frac{\partial(x,y,z)}{\partial(t,\theta_{out},\varphi_{out})}$. Owing to the classical free motion of the detached electron in the square torus microcavity, the amplitude can be evaluated analytically and is finally given by [21]:

$$A_j=\frac{R_0}{R_0+L_j}, \tag{11}$$

L_j is the length of the j-th detached electron's closed orbit.

The function S_j is the classical action along the j-th closed orbit: $S_j=\oint \vec{p}_j\cdot d\vec{q}_j$. For our system, the collision between the detached electron and the microcavity is elastic, so the momentum remains a constant along a path connecting two successive reflections. Therefore, the classical action along the j-th closed orbit is proportional to the length of that orbit: $S_j=kL_j$.

μ_j is the Maslov index, which records phase shifts due to the reflections of the microcavity.

When the returning wave returns to the small sphere close to the nucleus, it can be approximated by an incoming plane wave:

$$(\psi)^j_{ret}(r)=N_j\, e^{i\vec{k}^j_{ret}\cdot\vec{r}}, \tag{12}$$

where N_j is a matching factor:

$$N_j=\frac{i4Bk\chi(\theta^j_{out},\varphi^j_{out})}{(k_b^2+k^2)^2}\frac{1}{L_j}e^{i(S_j-\mu_j\pi)}. \tag{13}$$

Substituting the above equations into Eq. (7) and carrying out the overlap integral, the oscillatory part of the photodetachment cross section can be obtained:

$$\sigma^{osc}(E)=\frac{16\pi^2B^2E}{c(E_b+E)^3}\sum_j\frac{1}{L_j}\chi(\theta^j_{out},\varphi^j_{out})\chi^*(\theta^j_{ret},\varphi^j_{ret})\sin(kL_j-\mu_j\pi). \tag{14}$$

The summation in the above formula includes all the detached electron's closed orbits. Since all the closed orbits lie in the x-y plane, the outgoing and returning polar angles for the electron's closed orbits are $\theta^j_{out}=\theta^j_{ret}=\pi/2$. Thus, the angular factor for the x, y polarized laser light can be simplified as [22]:

$$\begin{aligned}\chi_x(\theta^j_{out},\varphi^j_{out})\chi_x^*(\theta^j_{ret},\theta^j_{ret})&=\cos\varphi^j_{out}\cos\varphi^j_{ret}\\ \chi_y(\theta^j_{out},\varphi^j_{out})\chi_y^*(\theta^j_{ret},\theta^j_{ret})&=\sin\varphi^j_{out}\sin\varphi^j_{ret}\end{aligned} \tag{15}$$

Using the above formulas, the total photodetachment cross section for x-polarized light can be written as:

$$\sigma_x(E)=\sigma_0(E)+\frac{16\pi^2B^2E}{c(E_b+E)^3}\sum_j\frac{1}{L_j}\cos\varphi_{out}^j\cos\varphi_{ret}^j\sin(kL_j-\mu_j\pi)\,, \tag{16}$$

For *y*-polarized light,

$$\sigma_y(E)=\sigma_0(E)+\frac{16\pi^2B^2E}{c(E_b+E)^3}\sum_j\frac{1}{L_j}\sin\varphi_{out}^j\sin\varphi_{ret}^j\sin(kL_j-\mu_j\pi)\,. \tag{17}$$

In order to show the correspondence between the oscillatory structure in the cross section and the detached electron's closed orbits in the square torus microcavity, we perform the Fourier transformation (FT) of the photodetachment cross section. The Fourier variable conjugate to the momentum is the path-length of the trajectory. Therefore, we compute the Fourier transform of Eqs.(16-17):

$$F(L')=\int_{k_1}^{k_2}[\sigma(E)-\sigma_0(E)]\exp(-ikL')dk\,. \tag{18}$$

In the above formula, L' represents the length of classical closed orbits. In our calculations, we calculate $|F(L')|^2$. Our final calculation result is a collection of peaks centered near the length of each closed orbit.

3. Results and discussions

In the following calculation, we assume the length of the outer and inner side of the microcavity is: *a*=100a.u., *b*=50a.u.. Using Eqs.(16-17) and considering all the detached electron's closed orbits, we calculate the photodetachment cross section of H^- ion in the square torus microcavity. Firstly, we calculate the total photodetachment cross sections for different polarized laser light. The calculation results are given in Figs.9-10. Fig.9 shows the variation of the total photodetachment cross sections with the length of the detached electron's closed orbit, the laser light is polarized along *x*-axis. In contrast to the smooth curve without the microcavity, oscillatory structures appear in the cross sections, which are caused by the interference between the returning electron waves travelling along the closed orbit with the outgoing source waves. Besides, the oscillatory structures depend on the length of the detached electron's closed orbit sensitively. As the length of the closed orbit is small, the oscillating amplitude and frequency in the cross section are relatively small. As we increase the length of the closed orbit, the oscillatory structure in the cross section becomes complicated. The reason can be analyzed as follows: from Table I, we can see with the increase of the length of the closed orbit, the number of the closed orbit is increased correspondingly. For example, in Fig.9(a), we calculate the photodetachment cross section with the length of the closed orbit L≤500a.u.. Under this condition, only 9 closed orbits can contribute to the photodetachment cross section, therefore, the oscillating amplitude and frequency in the cross section are relatively small. As the length of the closed orbit is increased to L≤1000a.u. (Fig.9(b)), there is altogether 14 closed orbits, the oscillating amplitude and frequency in the cross section are increased a little compared to Fig.9(a). When L≤1500a.u., the number of the closed orbit is increased to 25; as L≤2000a.u., the number of the closed orbit is further increased to 33. With the increase of the number of the closed orbit, the returning waves reflected back by the inner and outer surfaces of the square torus microcavity become increased greatly, which lead to the complicated oscillation in the photodetachment cross section. As we further increase the length of the closed orbit, the number of the closed orbit becomes increased correspondingly. The more the closed orbit, the more the returning waves bounced back by the surfaces of the microcavity; therefore, the oscillatory structure in the photodetachment cross section will become much more complex. As we can see from Figs.9(c-f) clearly.

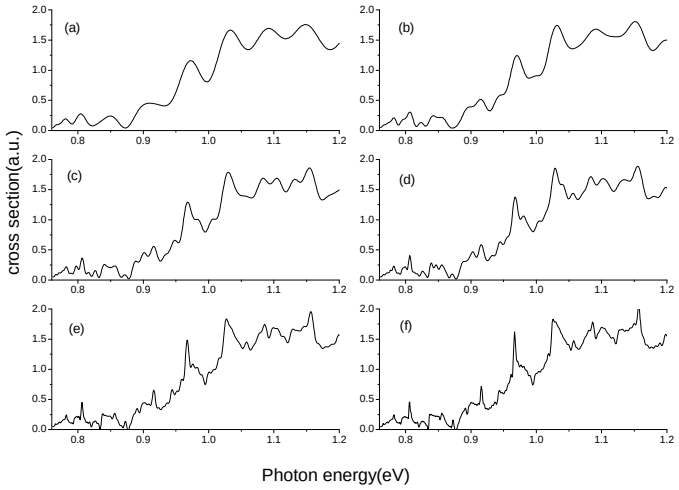

Fig.9. The photodetachment cross section of H^- ion in the square torus microcavity with different length of the closed orbit. The laser is linearly polarized in the x-direction. (a) L≤500a.u.; (b) L≤1000a.u.; (c) L≤1500a.u.; (d) L≤2000a.u. ; (e) L≤3000a.u.; (f) L≤5000a.u..

Fig.10 shows the total photodetachment cross sections of H^- ion in the square torus microcavity with the laser light polarized along *y*-axis. The lengths of the closed orbit are the same as those given in Fig.9. From this figure we also find as we increase the length of the closed orbit, the oscillatory structure in the cross section becomes much more complicated. However, in comparison with Fig.9, we find the oscillatory structures in the cross section are changed for different laser polarization. The oscillating amplitude in the cross section for the *y*-polarized laser light is a little smaller than the case for the *x*-polarized laser light. The reason is as follows: From Eq.(16) and Eq.(17), we find for different polarized laser light, the angular factor in the cross section is different. For the first kind closed orbit, the outgoing angles φ_{out}=0. This kind of closed orbit will have a significant contribution to the cross section for the *x*-polarized laser light. However, for the *y*-polarized laser light, we find as φ_{out}=0, the factor $\sin\varphi_{out}$ in the oscillating cross section is also 0, therefore, its contribution to the cross section disappears.

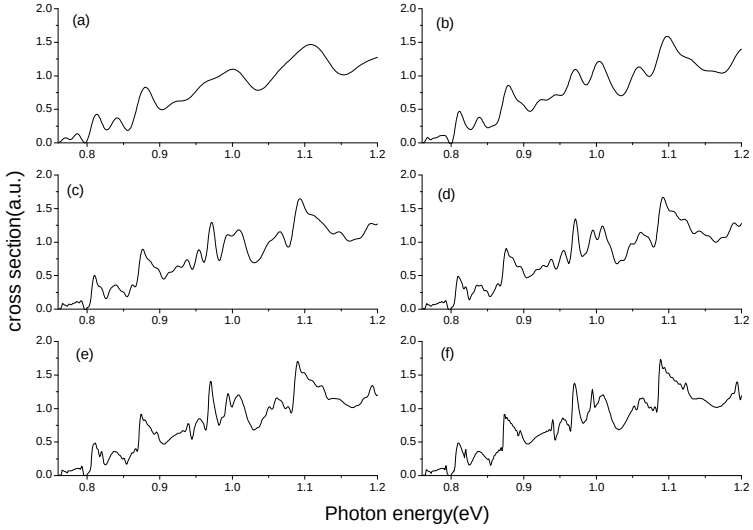

Fig.10. Variation of the photodetachment cross section of H^- ion in the square torus microcavity with different length of the closed orbit. The laser light is polarized in the y-direction. (a) L≤500a.u.; (b) L≤1000a.u.; (c) L≤1500a.u.; (d) L≤2000a.u.; (e) L≤3000a.u.;(f)L≤5000a.u..

In order to see the contribution of different kind of closed orbit to the photodetachment cross section, we calculate the oscillating part in the cross section with the length of the closed orbit L≤2000a.u.. The results are given in Figs.11-12. Fig.11 shows some typical oscillatory patterns caused by different kind of closed orbit, the laser light is polarized along *x*-direction. Fig.11(a) is the total oscillating part in the cross section. Figs.11(b-h) are the cross section corresponding to the seven kind of detached electron's closed orbits as we discussed in Section 2. From this figure, we find different kind of closed orbits lead to different structures. For the cross section corresponds to the first kind of closed orbit, the oscillating structure is relatively smooth but its amplitude is relatively large, so its contribution to the total oscillating cross section is significant. In addition, the contribution of the electron orbit with a small outgoing angle to the cross section is extremely complex, like the case of the second, fifth and sixth kind of closed orbit as we show in Fig.11(c,f,g). Both the oscillating amplitude and frequency in the cross section are relatively large. These kind of closed orbits make a strong modulation for the oscillating cross section. However, those electron's closed orbits with larger outgoing angles give only a weak oscillating pattern in the cross section and their contribution to the cross section are relatively small, like the case of the third , fourth and seventh kind of closed orbits as we show in Figs.11 (d,e, h).

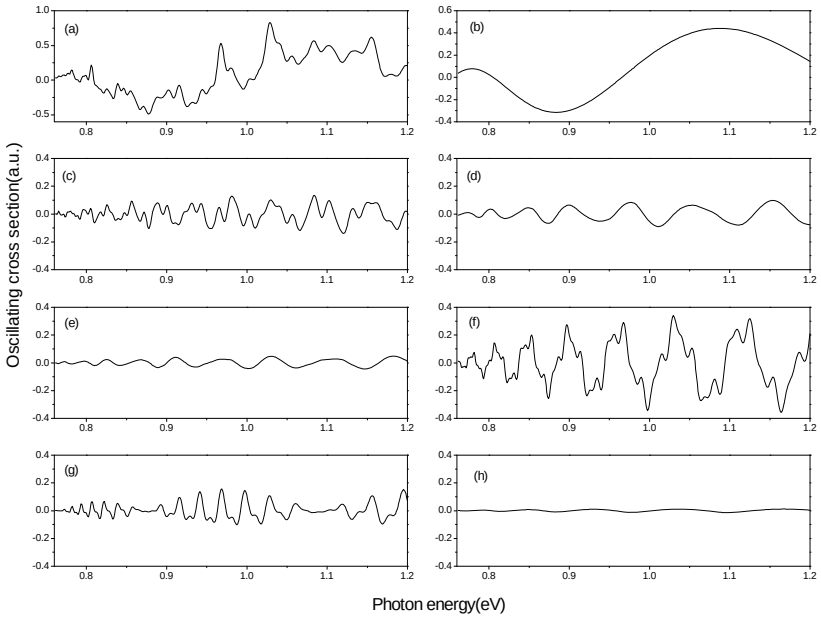

Fig.11. Some typical oscillatory patterns caused by different kind of closed orbit in the cross section, the length of the closed orbit L≤2000a.u.. The laser light is polarized along x-direction. (a) the total oscillating part in the cross section; (b-h) the cross section corresponding to the first, second, third, fourth, fifth, sixth and seventh kind of detached electron's closed orbits, respectively.

Fig.12 shows the contribution of different kind of closed orbit to the oscillating photodetachment cross section for the laser light polarized along *y*-direction. We find the contribution of the first kind of closed orbit to the cross section disappears. The second, fifth and sixth kind of closed orbits, whose outgoing angles are small, which makes their contribution to the cross section are extremely weak. In contrast, the contributions of the third , fourth and seventh kind of closed orbits to the cross section are relatively large, as we can see from Figs.12(d,e, h) clearly.

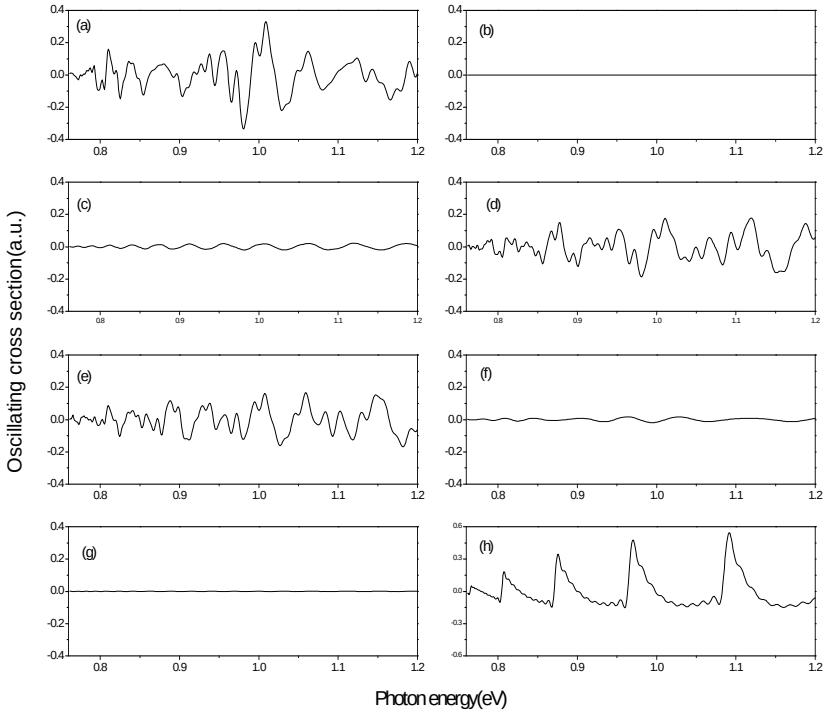

Fig.12. Some typical oscillatory patterns in the cross section caused by different kind of closed orbit, the length of the closed orbit L≤2000a.u.. The laser light is polarized along y-direction. (a) the total oscillating part in the cross section; (b-h) the cross section corresponding to the first, second, third, fourth, fifth, sixth and seventh kind of detached electron's closed orbits, respectively.

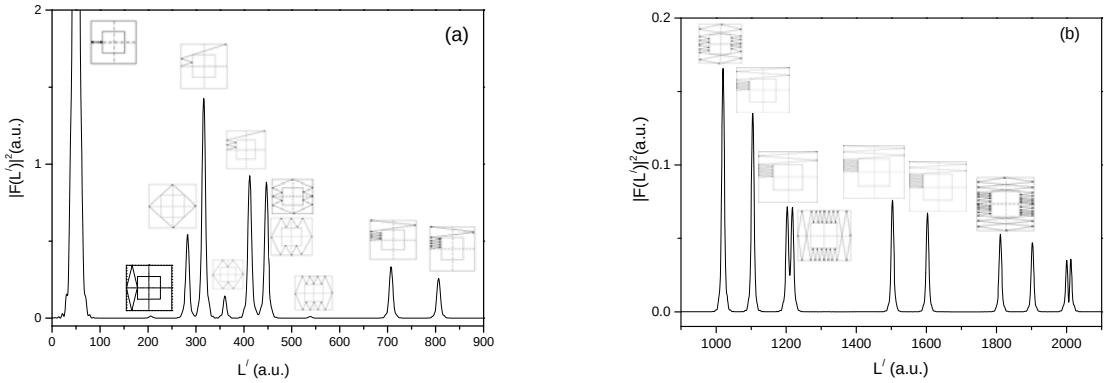

Fig.13. The Fourier transformed photodetachment cross section of H^- ion inside a square torus microcavity. (a) 0< L' ≤900 a.u.; (b) 900≤ L' ≤2100a.u.

Finally, we confirm the characteristics of quantum and classical correspondence in the square torus microcavity by calculating the Fourier transformation of the cross section. Suppose the laser light is polarized along the *x*-axis. The result is given in Fig.13. A series of peaks appear in the Fourier transformed cross section and each peak corresponds to the length of one detached electron's closed orbit. Some typical closed orbits are shown beside each peak. Fig.13(a) shows the Fourier-transformed cross section in the square torus microcavity with the length of the closed orbit 0< L' ≤900 a.u.. Fig.13(b) shows the Fourier-transformed cross section with the length of the

closed orbit $900 \leq L' \leq 2100$ a.u.. It is clearly seen that there are many sharp peaks at the lengths corresponding to the detached electron's closed orbit. The lengths of the closed orbits can be found in Table I.

4. Conclusions

We have thoroughly studied the photodetachment of H^- ion in the square torus microcavity on the basis of the semiclassical closed orbit theory. Taking the square torus microcavity with the side ratio of the inner and outer square equals to 0.5 as an example, we search out the detached electron's closed orbits and calculate the photodetachment cross section. The photodetachment cross section exhibits three main features. First, the oscillating amplitude and frequency in the photodetachment cross sections have a strong dependence on the length of the detached electron's closed orbit. With the increase of the length of the electron's closed orbit, the number of the closed orbit becomes increased, which makes the oscillatory structure in the photodetachment cross section becomes complex. Second, the total photodetachment cross section of H^- ion in the square torus microcavity is related to the laser polarization sensitively. Third, each peak in the Fourier-transformed photodetachment cross section corresponds to the length of one detached electron's closed orbit. This discovery demonstrates the quantum and classical correspondence in the square torus microcavity. In this work, we have made the calculation by assuming that the negative ion lies inside the concentric square torus microcavity. As to the photodetachment of H^- anion in the non-concentric square tours microcacity, the detached electron's motion will become more complex. In our future work, we will further study the photodetachment of anion in the non-concentric square tours microcacity. At present, with the development of negative ion photodetachment microscopy experiments, the studies of ion-microcavity interaction become increasingly important. Our studies may have potential applications in the surface chemistry and analysis, reactive ion etching, escape and transport, photodetachment microscopy experiment, etc.

Acknowledgements

This work is supported by the National Natural Science Foundation of China (Grant Nos.11374133 and 11074104), a Project of Shandong Province Higher Educational Science and Technology Program of China (Grant No. J13LJ04), and Taishan scholars project of Shandong province（ts2015110055).

References

[1] G. C.Yang, Y. Z. Zheng, X. X. Chi, J.Phys.B **39,** 1855 (2006).
[2] G. C.Yang, Y. Z. Zheng, X. X.Chi, Phys. Rev.A **73,** 043413 **(**2006).
[3] D. H. Wang, Eur.Phys.J.D **45,** 179 (2007).
[4] A. Afaq, M. L. Du, J.Phys.B **40,** 1309 (2007).
[5] H. J. Zhao, M. L. Du, Phys. Rev.A **79,** 023408 (2009).
[6] K. K. Rui, G. C. Yang, Surf. Sci. **603**, 632 (2009).
[7] B. C.Yang, M. L.Du, J. Phys. B **43,** 035002 **(**2010).
[8] T. T. Tang, D. H. Wang, J. Phys. Chem. C **115,** 20529 (2011).
[9] Y. Han, L. F. Wang, S. Y. Ran, G.. C. Yang, Phys. B **405,** 3082 (2010).
[10] K. Y. Huang, D. H. Wang, J. Phys. Chem. C **114,** 8958 **(**2010).
[11] D. H. Wang, J. Appl. Phys. **109,** 014113 **(**2011).
[12] D. H. Wang, S. S. Wang, T. T. Tang, J. Phys.Soc.Jpn. **80,** 094301 **(**2011).
[13] M. Haneef, I. Ahmad, A. Afaq, A. Rahman, J. Phys. B **44**, 195004 **(**2011).
[14] D. H. Wang, S. S. Li, H. F. Mu, J. Phys.Soc.Jpn. **81**, 074301 (2012).
[15] D. H. Wang, Curr. Appl. Phys. **11**, 1228 **(**2011).
[16] P. Hansen, K. A. Mitchell, J. B. Delos, Phys. Rev. E **73,** 066226 **(**2006).
[17] J. Novick, M. L. Keeler, K. J. Giefer, J. B. Delos, Phys. Rev. E **85,** 016205 (2012).
[18] J. Novick, J. B. Delos, Phys. Rev. E **85,** 016206 (2012).
[19] K. A. Mitchell, J. P. Handley, B. Tighe, A. Flower, J. B.Delos, Phys. Rev. Lett. **92**, 073001 (2004).
[20] K. A. Mitchell, J. P. Handley, B. Tighe, A. Flower, J. B. Delos, Phys. Rev. A **70**, 043407 (2004).
[21] H. J. Zhao, M. L. Du, Phys. Rev.E **84,** 016217 (2011).
[22] D. H. Wang, S. S .Li, Y. H. Wang, H. F. Mu, J. Phys.Soc.Jpn. **81**, 114301 (2012).
[23] D. H. Wang, S. Liu, Y. H. Wang, Chin. Phys. B **22**, 073401 (2013).
[24] D. H.Wang, Chin.J.Phys. **52**, 138 (2014).
[25] P. H. Tuan, Y. T. Yu, P. Y. Chiang, H. C. Liang, K. F. Huang, Y. F. Chen, Phys. Rev. E **85,** 026202 (2012).
[26] M. L. Du, J. B.Delos, Phys. Rev. A **38,** 1896 **(**1988).
[27] A. D. Peters, J. B.Delos, Phys. Rev.A **47,** 3020 **(**1993).
[28] M. L. Du, Phys. Rev.A **70,** 055402 **(**2004).

*Corresponding author: lduwdh@163.com